Evidence for resonant bonding in phase-change materials studied by IR spectroscopy

K. Shportko[1], H. Volker[2], M. Wuttig[2]
[1]*V. Lashkaryov Institute for Semiconductor Physics, NAS of Ukraine,*
41, prospect Nauky, 03680 Kyiv, Ukraine, e-mail: konstantin@shportko.com
[2]*I. Institute of Physics (IA), RWTH University of Technology Aachen,*
Sommerfeld str. 14, Aachen 52056, Germany

Abstract. Phase-change materials (PCM) attract attention due to their unique properties. This remarkable portfolio also makes them promising for applications in novel data storage devices. In this study, we discuss differences in the optical properties of PCM and non-PCM in the IR caused by presence or absence of resonant bonding.

Keywords: phase-change materials, resonant bonding, optical properties.

1. Introduction

Electronic memories utilize a pronounced change in resistance to store information. At present, dynamic random access and flash memories are the two implementations of choice in the IT industry. Both face scaling problems and have rather different attributes. This has motivated the search for alternatives. Already in the 1960s, S. Ovshinsky suggested to use rapid phase transitions from amorphous to crystalline states in some chalcogenide alloys (later called "phase-change materials" (PCM)) for memory applications [1]. These materials have recently been introduced in the memory market by companies like Samsung (www.samsung.com) and Micron (www.micron.com).

PCM, which include Ge-Sb-Te (GST) alloys, exhibit a remarkable difference of their electrical and optical properties in the amorphous and crystalline states. Their application potential originates from this property contrast and the ability to rapidly re-switch between these states. Currently, PCM are widely used in optical data storage and considered to be promising for non-volatile memory technology [2]. Thus, the fundamental understanding of properties of the phase change alloys might hold significant promise for material optimization in next generation storage devices.

In modern chemistry, the idea of resonance between equivalent valence-bond configurations, as put forward by Pauling [3], is a generally accepted concept crucial for understanding many molecules such as benzene. While resonance has been considered in the description of solids as early as 1957 [4], it has become more widely recognized after 1973 especially through the works of Lucovsky and White [5] and of Littlewood [6] on IV-VI compounds, in which 6-fold coordination accompanies bonding by three *p*-electrons per atom.

In our previous study [7], we have reported the difference of 70–200% of the optical dielectric constant between the crystalline and the amorphous phases of PCM, which is attributed to a significant change in bonding type between the two phases. We suggested that PCM in the crystalline phase utilize the resonant bonding, which explains the following contrast of properties. The optical dielectric constant of the amorphous phases is that expected of a covalent semiconductor, whereas that of the crystalline phases is strongly enhanced by resonant bonding effects. In addition, the sub-gap (Drude-like) absorption by free

charge carriers in the crystalline phase and the larger bandgap of the amorphous phase were reported [7].

Meta-stable GSTs crystallize in the distorted rock-salt structure with the anion sub-lattice occupied by Te atoms, whereas the cation sub-lattice is randomly occupied by Ge atoms, Sb atoms and empty lattice sites (for example, 12,5% and 10% for $Ge_1Sb_2Te_4$ and $Ge_2Sb_2Te_5$, respectively) [8, 9]. In this work, we have chosen the following PCM: $Ge_1Sb_2Te_4$ (GST124), $Ge_2Sb_1Te_4$ (GST214), $Ge_2Sb_2Te_4$ (GST224), $Ge_2Sb_2Te_5$ (GST225), $Ge_3Sb_2Te_6$ (GST326), $Ge_3Sb_4Te_8$ (GST348), GeTe with resonant bonding and compare their properties with covalently bonded non-PCM: InSb, $AgInTe_2$ (AIT), GeSe and SnSe. To show the difference between these two classes of materials, we applied the Moss rule that combines the optical dielectric constant ε_∞ and the band gap E_g in the following way [7]:

$$\varepsilon_\infty^2 E_g \approx \text{const.} \qquad (1)$$

The data of the amorphous and the crystalline covalently bonded non-PCM, as well as that of the both states of the PCM, exhibits the significant contrast between these two classes of materials. The difference in the $\left(\varepsilon_\infty^2 E_g\right)_{cr} / \left(\varepsilon_\infty^2 E_g\right)_{am}$ ratio presented in Fig. 1 is caused by the fact that amorphous PCM possess systematically lower values of Moss "constants" than those in the corresponding crystalline state, which is not the case for non-PCM. This evidence can be explained by the change of bond type upon crystallization of PCM. This behaviour separates PCM from other covalently bonded materials, which do not reveal such a significant property contrast between both states. This is in line with Lucovsky and White, who have reported that materials with resonant bonding in the crystalline phase exhibit a property contrast with the corresponding amorphous phase [5].
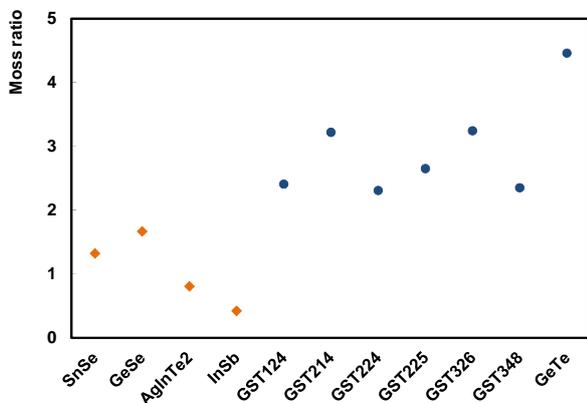

Fig. 1. The ratio $\left(\varepsilon_\infty^2 E_g\right)_{cr} / \left(\varepsilon_\infty^2 E_g\right)_{am}$ of non-PCM (brown squares) and PCM (blue circles).

This work is aimed to examine evidences of the resonant bonding in GSTs, which can be found beyond the spectral range reported in [7], namely, in the range of the phonon modes (below 0.025 eV) and interband electron transitions (around 3 eV).

2. Experimental details

In this work, we have studied samples of PCM and non-PCM in the amorphous and crystalline phases. The investigated samples were prepared in the form of thin films in the following way: a 150-nm Al layer was deposited onto a glass substrate. After that, the PCM or non-PCM film (1,000 nm) was d.c. sputter deposited onto it. To obtain the polycrystalline samples, the as-deposited amorphous films were annealed in Ar atmosphere for 30 min at temperatures about 10 °C above their corresponding crystallization temperatures. In our experiments, we used meta-stable crystalline GST samples with distorted rock-salt structure. The structure of the studied samples was checked by X-ray diffraction. The layer thickness was determined on reference samples prepared in the same sputter session using a Bruker Dektak profilometer.

To study the dielectric function of selected materials, we applied FTIR spectroscopy. IR reflectance spectra were measured within the range 4 to 40 meV and from 0.5 to 2 eV, using a Bruker IFS 66v/s spectrometer with a Hg lamp and a globar as the radiation sources as well as DTGS detector. A gold mirror (300 nm thick layer of gold, deposited on glass) with a reflectance index of 0.99 in the IR was used as a reference for reflectance measurements. The angle of incidence of radiation is about 10 and taken into account in calculations of the reflectance spectra.

FTIR reflectance spectra were fitted using SCOUT software. To model the phonons' contribution to the dielectric function, we used the Kim model, which is a mixture of Lorentz and Gauss profiles [10]. To fit the spectra in the range of the electron interband transitions the Tauc–Lorentz oscillator was used in the model of the dielectric function [11].

3. Results and discussion

We start with the analysis of the influence of the resonant bonds on the dielectric function in the range of the electron interband transitions. When discussing the consequences of application of the Moss rule to the non-PCM and PCM, we took the position of the optical absorption edge for the input parameter E_g. In what follows, we particularly focus on the behaviour of the imaginary part of their dielectric function around this range.

Fig. 2 displays ε_2 around the electron interband transitions, which cause absorption above 0.5 eV. As mentioned in the Experimental section, we used a Tauc–Lorentz oscillator to model this increase of the

imaginary part of their dielectric function around this range. It is interesting that this simple model is sufficient, except for the position of the absorption edge, which has been discussed in [7]. The peak value of ε_2 exhibits significant differences between the amorphous and crystalline state of PCM. This is in contrast to the case of non-PCM, where the position of the absorption edge and peak value of ε_2 are of the same order for both crystalline and amorphous state. This feature can also be seen in the data of GST225 presented in [12], however, it was not explained there.

According to the concepts of quantum mechanics, ε_2, the imaginary part of the dielectric function in the range of the interband transition is related with the matrix element [13] that can be calculated employing Fermi's golden rule [14]:

$$\lambda_{if} = \frac{2\pi}{\hbar}\left|M_{if}\right|^2 \rho_f , \qquad (2)$$

where λ_{if} is the transition probability, $\left|M_{if}\right|$ – matrix element for the transition and ρ_f – joint density of states. The joint density of states hardly changes upon crystallization. It is confirmed by DFT calculations and XPS/UPS experiments [15]. Therefore, the significant contrast in ε_2 for PCM between the amorphous and crystalline state (~2 times) can be only explained by the increase of the transition matrix element in PCM upon crystallization. This statement is supported by data for non-PCMs, which show no change in bonding upon crystallization and, therefore, possess values of the ratio $\left(\varepsilon_{2\,max}\right)_{cr}/\left(\varepsilon_{2\,max}\right)_{am}$ around 1, as shown in Fig. 3.
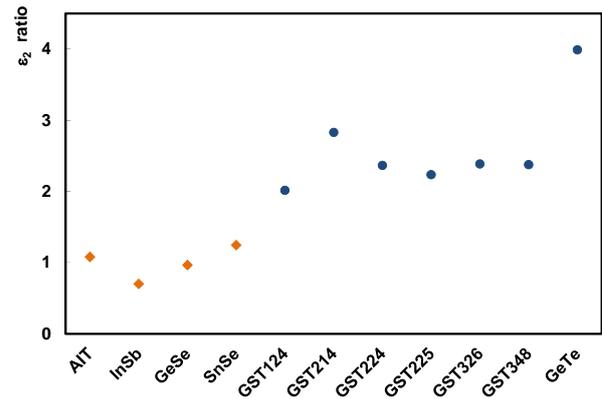
Fig. 3. The ratio $\left(\varepsilon_{2\,max}\right)_{cr}/\left(\varepsilon_{2\,max}\right)_{am}$ for the non-PCM (brown squares) and PCM (blue circles).

Further, we will focus on the next aspect: the consequences of the presence of resonant bonding in the crystalline PCM on their dielectric function in the range of phonon modes. To facilitate the analysis of these consequences, an influence of crystallization on the dielectric function of the conventional semiconductor material AIT in this specific spectral range was first considered.

The imaginary part of the dielectric function ε_2 of non-PCM AIT in the 0.004-0.04 eV range is shown in Fig. 4 (Inset A). Being compared with the amorphous phase, the crystalline one in AIT displays: i) a similar profile of ε_2, which means identical phonon absorption peaks arrangement, due to the similar short-range order and similar bonding type in both phases, ii) sharper and
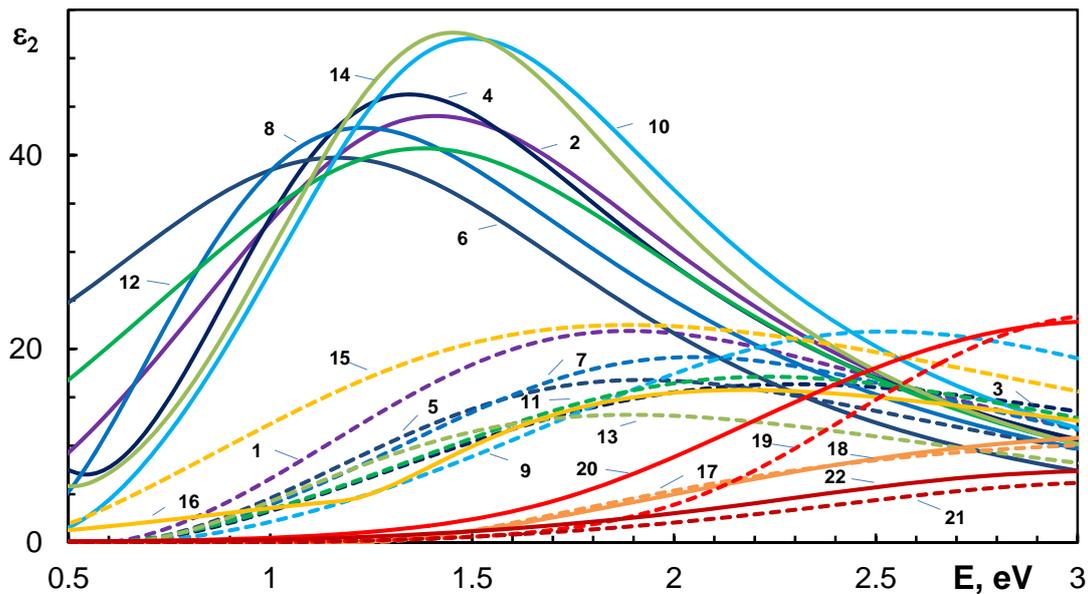
Fig. 2. Imaginary part of the dielectric function ε_2 of PCM and non-PCM in the range of the electron interband transitions. PCM: *1* – GST124 am, *2* – GST124 cr, *3* – GST214 am, *4* – GST214 cr, *5* – GST 224 am, *6* – GST224 cr, *7* – GST225 am, *8* – GST225 cr, *9* – GST326 am, *10* – GST326 cr, *11* – GST348 am, *12* – GST348 cr, *13* – GeTe am, *14* – GeTe cr; non-PCM: *15* – InSb am, *16* – InSb cr, *17* – AIT am, *18* – AIT cr, *19* – GeSe am, *20* – GeSe cr, *21* – SnSe am, *22* – SnSe cr.

higher phonon absorption peaks due to the presence of long-range order, absent in the amorphous phase.

In contrast to AIT, we observe three significant differences between ε_2 of amorphous and crystalline phases in GST225 shown in Fig. 4: i) a different pattern of ε_2, ii) phonon absorption peaks of the crystalline GST225 are located at lower energies than those of the corresponding amorphous state, and iii) huge difference (10 times) in the intensities of phonon absorption peaks, which cannot be only explained by acquisition of the long-range order upon crystallization. Furthermore, the shift of the phonon absorption peaks and the difference in their intensities between amorphous and crystalline states correlate with the stoichiometry (Fig. 4, Inset B): both effects are more pronounced in GST326 and less pronounced in GST124, respectively.

The observed phenomena can be explained in the terms of resonant bonding. The difference in the profile of ε_2 is shown in Fig. 4 can be attributed to different local atomic arrangement in the amorphous and crystalline states of PCM [16]; larger coordination number, longer bond length and larger coefficient of thermal expansion explain softening the phonon modes in the crystalline states of PCM [17]. These two phenomena provide evidence that the bonding type in the crystalline state of PCM is not the same as that inherent to the amorphous state, *i.e.*, covalent bonding. An important feature of the resonant bonding is that the electron density distribution is highly delocalized [5]. As a result, the materials of this group possess high Born effective charges [18], as well as a large electronic polarizability and dielectric constants [7]. In [19–22], it

has been shown that the intensities of the IR active modes (and corresponding oscillator strengths) are related with the Born effective charge.

Thus, the difference in the intensities of the IR active phonon peaks in PCM is an experimental evidence of the much higher Born effective charge in the crystalline phase. Systematic variation of the stoichiometry of the studied GST alloys (increase of the Ge content) lowers the concentration of the vacancies in studied materials and, therefore, is responsible for the stoichiometry-related dependence in Fig. 4 (Inset B): materials with lower vacancy concentration exhibit higher intensities of the IR active modes and, consequently, higher Born charges.

4. Conclusions

Full utilization of the potential inherent to these PCM requires the comprehensive understanding of their properties. Crystalline PCM can be separated from other semiconductor materials due to their unique properties portfolio. In this study, we have shown that resonant bonding in crystalline PCM influences their dielectric function in the range of the IR active phonons and the interband electron transitions.
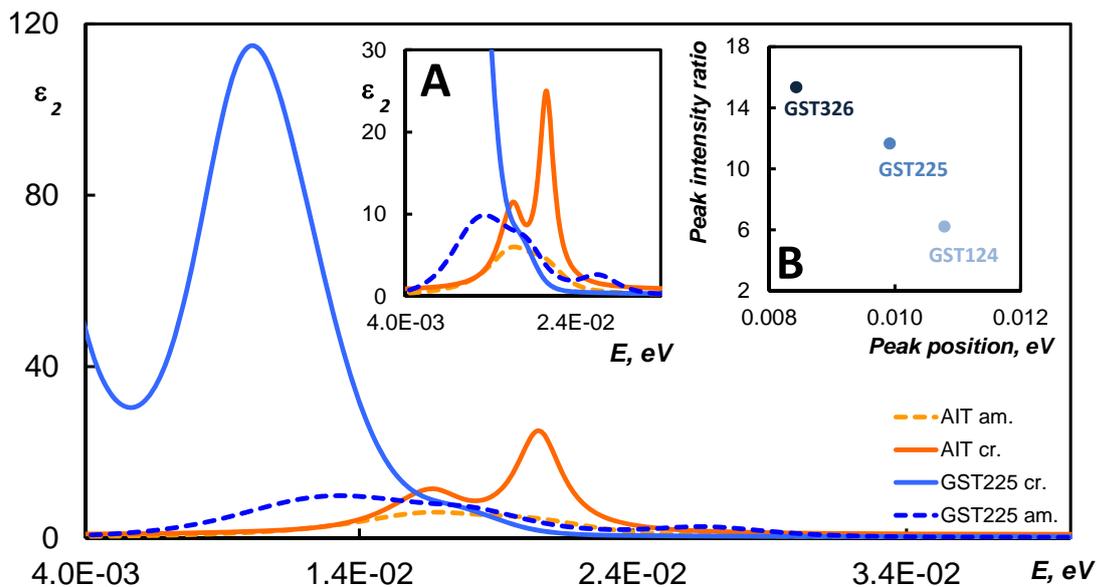
Acknowledgements

Fig. 4. Imaginary part of the dielectric function ε_2 of non-PCM (AIT) and PCM (GST225) in the range of phonon modes. (Inset A. Magnification of ε_2 for amorphous and crystalline AIT as well as amorphous GST225; Inset B. Crystalline GST: the ratio $\left(\varepsilon_{2\,max}\right)_{cr}/\left(\varepsilon_{2\,max}\right)_{am}$ vs. corresponding peak positions.)

Scalability'.

References

1. Ovshinsky S.R. Reversible electrical switching phenomena in disordered structures. *Phys. Rev. Lett.* 1968. **21**. P. 1450.
2. Wuttig M. Phase change materials: Towards a universal memory? *Nat. Mater.* 2008. **4**. P. 265–266.
3. Pauling L. *The Nature of the Chemical Bond*, 3-rd ed. Cornell University Press, 1970.
4. Krebs H. Der Einfluß homöopolarer Bindungsanteile auf die Struktur anorganischer Salze. III Verbindungen der Halbmetalle. *Zeitschrift für Elektrochemie, Berichte der Bunsengesellschaft für Phys. Chemie.* 1957. **61**. P. 925–934.
5. Lucovsky G. and White R.M. Effects of resonance bonding on the properties of crystalline and amorphous semiconductors. *Phys. Rev. B.* 1973. **8**, No. 2. P. 660–667.
6. Littlewood P.B. The crystal structure of IV-VI compounds. I. Classification and description. *J. Phys. C Solid State Phys.* 1980. **13**. P. 4855.
7. Shportko K., Kremers S., Woda M., Lencer D., Robertson J., and Wuttig M. Resonant bonding in crystalline phase-change materials. *Nat. Mater.* 2008. **7**, No. 8. P. 653–658.
8. Zalden P. *et al.* Specific heat of $(GeTe)_x (Sb_2Te_3)_{1-x}$ phase-change materials: The impact of disorder and anharmonicity. *Chem. Mater.* 2014. **26**, No. 7. P. 2307.
9. Siegrist M., Jost T., Volker P., Woda H., Merkelbach M., Schlockermann P., Wuttig C. Disorder-induced localization in crystalline phase-change materials. *Nat. Mater.* 2011. **10**. P. 202–208.
10. Kim P.M., Garland C.C., Abad J.W., Raccah H. Modeling the optical dielectric function of semiconductors: Extension of the critical-point parabolic-band approximation. *Phys. Rev. B.* 1992. **45**, No. 20. P. 11749–11767.
11. Jellison G.E., Jr. Spectroscopic ellipsometry data analysis: measured versus calculated quantities. *Thin Solid Films*. 1998. **313–314**. P. 33–39.
12. Shimakawa K., Střižik L., Wagner T., and Frumar M. Penn gap rule in phase-change memory materials: No clear evidence for resonance bonds. *APL Mater.* 2015. **3**, No. 4. P. 41801.
13. Van Dyke J.P. Matrix elements in interband optical transitions. *Phys. Rev. B.* 1972. **5**, No. 4. P. 1489–1493.
14. Bransden C.J., Joachain B.H. *Quantum Mechanics*, 2nd ed. Harlow: Pearson Education Limited, 1999.
15. Wełnic W., Botti S., Reining L., and Wuttig M. Origin of the optical contrast in phase-change materials. *Phys. Rev. Lett.* 2007. **98**, No. 23. P. 236403.
16. Shportko K., Venger E. Influence of the local structure in phase-change materials on their dielectric permittivity. *Nanoscale Res. Lett.* 2015. **10**, No. 33.
17. Matsunaga T. *et al.* Phase-change materials: Vibrational softening upon crystallization and its impact on thermal properties. *Adv. Funct. Mater.* 2011. **21**, No. 12. P. 2232–2239.
18. Lencer D., Salinga M., Grabowski B., Hickel T., Neugebauer J., and Wuttig M. A map for phase-change materials. *Nat. Mater.* 2008. **7**, No. 12. P. 972–977.
19. Brüesch P. *Phonons: Theory and Experiments III*. vol. 66. Berlin, Heidelberg: Springer, 1987.
20. Giannozzi P., Baroni P. Vibrational and dielectric properties of C60 from density-functional perturbation theory. *J. Chem. Phys.* 1994. **100**, No. 11. P. 8537–8539.
21. Gonze X. and Lee C. Dynamical matrices, Born effective charges, dielectric permittivity tensors, and interatomic force constants from density-functional perturbation theory. *Phys. Rev. B.* 1997. **55**, No. 16. P. 10355–10368.
22. Chen I. and Zallen R. Optical phonons and dynamic charge in trigonal Se and Te. *Phys. Rev.* 1968. **173**, No. 3. P. 833–843.